Energy Conversion and Management 307 (2024) 118350

Contents lists available at ScienceDirect

Energy Conversion and Management

journal homepage: www.elsevier.com/locate/enconman

Extended exergy analysis of a novel integrated absorptional cooling system design without utilization of generator for economical and robust provision of higher cooling demands

Asli Tiktas [a], Huseyin Gunerhan [b], Arif Hepbasli [c,*], Emin Açıkkalp [d]

[a] Department of Mechanical Engineering, Faculty of Engineering-Architecture, Kırşehir Ahi Evran University, 40100 Bağbaşı, Kırşehir, Turkey
[b] Department of Mechanical Engineering, Faculty of Engineering, Ege University, 35100 Bornova, Izmir, Turkey
[c] Department of Energy Systems Engineering, Faculty of Engineering, Yasar University, 35100 Bornova, Izmir, Turkey
[d] Department of Mechanical Engineering, Faculty of Engineering, Eskisehir Technical University, 26555 Eskisehir, Turkey

ARTICLE INFO

Keywords:
Absorptional cooling cycle
Solar energy
Absorptional heat transformer
Extended exergy analysis
Environmental impact assessment

ABSTRACT

The focus of this study is on designing a novel system for the provision of high-capacity cooling and heating loads (4000 kW) with the utilization of absorption technology to increase economic viability and COP value of existing cooling plants via lower-grade waste heat sources (70 °C-90 °C). To achieve this aim, in the novel system, an integration including the LiBr-water solution based absorptional heat transformer (AHT), and absorptional cooling cycle (ACC), and flat plate solar collector (FPSC) systems was proposed. In the integration, the utilization of the generator in the cooling cycle was avoided with the interaction of the high-temperature LiBr-water solution (120 °C-150 °C) from the AHT system and ACC system evaporator. In this way, both the additional cost of the boiler and heat source and the enhancement of economic viability and COP value were achieved. Energy, economic, traditional, and extended exergy, sustainability, and environmental analyses were implemented in this novel system. The COP value for the cooling system was determined to be 3.10 from energy analysis. This result forms a significant indicator for achieving of the main focus of the current study with the proposed novel system. The annual heating and cooling duty generations with this novel system were computed as 52.37 GWh and 52.40 GWh, respectively. In the context of economically comparing the proposed system to other plants with similar scale that already exist, the initial overall expenditure, yearly operational expenses, and the time it takes to recover the investment for the proposed system were set at $4.56 million, $3.12 million, and 1.75 years, respectively. It is worth noting, though, that these figures fall within the range of $6–8 million, $5–7 million, and 5–10 years, respectively, for the currently operational plants. This result indicated that the proposed system provides a robust alternative to the existing cooling-heating cogeneration systems in terms of main output generation and is more economically viable. Also, the novel system gained annually US$3.89 million in energy costs. The conventional exergy analysis results were summarized by forming an exergy flow and loss diagram, namely, the Grassmann diagram. In addition, in this current study, the novel extended exergy flow diagram indicating extended exergy content components, energy carriers of the proposed system, and exergy product rate streams was also proposed and drawn for the proposed system.

1. Introduction

In the energy outlook report of 2023 published by BP [1], it was stated that Russia's invasion of Ukraine reversed the trend of recession in the energy sector with the COVID-19 pandemic process [1]. Depending on the intense market fluctuations in natural gas and oil supply, the renewable energy investment rate, which was 15 % in 2021, is expected to reach 24 % this year. But at the same time, the report states that despite the high rate of increase in renewable energy utilization, fossil fuels continue to maintain 82 % of global primary energy consumption. Considering the tendency of this share, which was 87 % in 2010, to decrease to 82 %, it is thought that 200 years are required for the fossil fuel consumption share to reach zero. Significantly reducing the share of fossil energy sources constitutes a sustainable solution to global-scale threats such as the energy crisis, increasing greenhouse gas

* Corresponding author.
E-mail address: arif.hepbasli@yasar.edu.tr (A. Hepbasli).

https://doi.org/10.1016/j.enconman.2024.118350
Received 13 January 2024; Received in revised form 10 March 2024; Accepted 23 March 2024
Available online 29 March 2024

Nomenclature

Abbreviations

ABS	Absorber
ACC	Absorptional cooling cycle
AHT	Absorptional heat transformer
Con	Condenser
EV	Evaporator
FPSC	Flat plate solar collector
Gen	Generator
P	Pump
SHX	Solution heat exchanger
V	Expansion valve

Symbols

adp.GWP	Environmental impact of a substance concerning its degradation in the atmosphere with respect to global warming
AEC	Yearly electricity usage measured in kilowatt-hours, kWh/year
ALR	Annual rate of substance leakage, measured in kilograms per year, kg/year
b	Exergy value per mole of a chemical compound, kW/mole
C	Substance charge mass causing emission, kg
CC	Capital cost, $
E	Equivalent exergy, kJ
$\dot{E}$	Exergy rate, kW
ee	Specific equivalent exergy, GJ/day
EE	Extended exergy, kJ
EEF	Factor quantifying the impact on the environment
EF	Emission factor associated with a plant's pollutant output
EcoEF	Ecological effect factor
Em	CO_2 emission, kg
EOL	End of life substance, years
Ex	Essential exergy consumption, MJ/person.day
ex^*	Vector of indices for cumulative exergy consumption
ExSI	Exergetic sustainability index
ExWR	Fuel exergy waste ratio
f	Consumption correction factor related to the modern standard of living
F	Numerical values representing the production relationships between energy carriers and materials as secondary products
GWP	Impact or potential of a substance or activity to contribute to global warming or climate change
h	Amount of enthalpy, expressed in kilojoules per kilogram, kJ/kg, for a specific substance or system
L	Duration of existence or longevity, typically measured in years
$\dot{m}$	Mass flow rate, kg/s
MM	Equivalent CO_2 emission associated with the manufacture of 1 kg of material
m	Material mass, kg
mr	Recycled material mass, kg
N	Total number of components
$\dot{Q}$	Heat transfer rate, kW
RDF	Substance disposal emissions, kg
RM	Equivalent CO_2 emission pertained with the recycling of 1 kg material, recycled material mass, kg
RMF	Amount of emissions generated during the production of a particular substance, measured in kilograms, kg
s	Measure of entropy for a specific substance, kJ/kg·K
SEF	Factor related to the interaction and interdependence between social and ecological systems
T	Temperature, ^{o}C or K
S	National monetary amount of wages and salaries, €/year
x	Weight percentage of lithium bromide (LiBr) in a solution or substance
z	Ratio of the number of moles of a specific component to the total number of moles in a mixture or solution, often expressed as a decimal or fraction

Subscripts

0	Dead-state
A	Coefficients of the consumption of energy carriers and materials
c	Capital
CEXC	Cumulative exergy consumption
D	External supplies
DD	Secondary production that does not contribute to or complement the primary or main production process
F	External supply that does not augment or support the primary production process
G	Main products
h	Human
E	Environmental remediation cost
eq.mfg	Equipment manufacturing
re.mfg	Substance manufacturing emissions
eq.rcy	Equipment recycling
ex	Exergetic
F	Fuel
k	Equipment
L	Labor
m	Material
surv	Human survival
wh	Workhour

Superscripts

Ch	Chemical
Ph	Physical

Greek letters

η	Efficiency

emissions, and environmental problems. This sought-after sustainable solution can only be achieved by integrating renewable energy sources with waste heat recovery systems in an effective way. According to the data of the International Energy Agency [2], the sector with the highest waste heat potential is the industry where 60 % of the global primary energy consumption is realized [2]. Absorption cooling systems are widely used to obtain the cooling load by considering the environmental emissions by making use of the waste heat in the industry at low temperature and high density [3–5]. However, studies in the literature have shown that waste heat source temperature should range from $120^{\circ}C$ to $175^{\circ}C$ to obtain high-capacity cooling loads with absorption cooling systems [6–8]. Since it is often not easy to reach the waste heat source in this temperature range, the absorption cooling system is used by integrating various sub-systems with high cost and complicated equipment. Therefore, the number of multigeneration systems based on such system designs is quite high in the literature [9–20].

In this regard, Mohan et al. [21] developed a trigeneration system that included the gas turbine, steam Rankine cycle, and air gap membrane distillation systems. The reason for designing this system was to produce electricity, clean water, and cooling loads with the utilization of

waste heat from gas turbine flue gases. Energy efficiency values of 82 %-85 % and COP values of 0.69–0.75 were obtained from this system with a total cost of US$11 million for 34 MW of electricity, 358 kg/s of clean water, and 4621 kW of cooling load. Kumar and Singh [22] evaluated a cogeneration system constituted of an ORC, gas turbine, solid-oxide fuel cell, and absorptional refrigeration systems for producing power and cooling loads. Thermal efficiencies of 60 %-73.8 %, specific work outputs ranging from 1095 to 1470 kJ/kg, and cooling loads of 14–23 tons were acquired with 1939.93 $/kW of unit power cost. Wang et al. [23] skeletonized a trigeneration system comprised of an ORC, Brayton, supercritical CO_2, absorptional cooling, and intercooler systems for power, heating, and cooling requirements. 36.02–43.67 MW of net power values, 3.84–6.79 MW of cooling values, and 9.55–12.66 MW of heating outputs were attained with total cost rates in the range of 0.597 and 0.777, thermal efficiencies of 49.19–63.65 %, exergy efficiency values of 43.46–51.94 %, and COP values of 0.571–0.613. Schüppler et al. [24] investigated cooling supply costs for universities around the world where high cooling load requirements exist to present an overview. They stated that the initial investment cost of the systems developed to meet the cooling needs only was in the range of US$4.5–7 million, and the annual cost of these systems varied between €4 and 7 million. The data obtained from this study agreed with the data specified in the Bowling Green State University central cooling [25], Cleveland Hopkins International airport chilled water [26], and ZEOSOL integrated solar heating and cooling plants report [27].

High total system costs (e.g., US$11 million for 4000 kW cooling) arise from demanding elevated waste heat temperatures (120 °C-175 °C) in integrated absorption cooling, per extensive literature [28–35]. In addition, it has been clearly seen that the COP value rarely approaches one in these integrated systems. This is due to the necessity of meeting the heat input requirements of the boiler in addition to the pumping power needed to obtain the cooling load. Hence, a substantial literature gap exists in efficiently addressing high cooling loads via integrated absorption systems with lower-grade waste heat sources (70 °C-90 °C) while enhancing economic viability and COP value.

The current research progresses mainly in two different ways. The one is a small-capacity cooling load production economically with lower-grade waste heat sources via compact system designs. For this aim, generally single-stage absorption cooling systems are utilized for lower pumping work and generator heat input requirements. However, the second way is the adoption of the concept of producing high-capacity cooling loads together with the numerous high-capacity production outputs such as heating loads, power, hydrogen, hot and fresh water, etc., by integrating different robust prime movers and heat sources. In this way, high-capacity production outputs are obtained from complex system designs and higher system installation and operation costs by utilizing higher-grade waste heat sources. This method requires a higher-grade waste heat source due to the production of high-capacity cooling loads. Hence, to reach this high temperature level, various fossil and renewable energy-based heat sources are combined. With the utilization of the fossil-based-heat sources, this temperature level is reached more easily while also having higher environmental impacts. In the situation of purely renewable energy-based heat source integration, not only is the speed of reaching the required temperature level slower, but achieving this brings with it high costs and complex system designs. Despite all these drawbacks, such system designs have been the subject of intense interest because they are important in terms of environmental impact and sustainability. For this reason, it becomes an important element to obtain a more feasible system by actively using effective waste heat mechanisms and interactions in these system designs. Therefore, in the systems designed within the scope of the second way, cycles with more complex designs are used instead of single-stage absorption cooling systems with low cooling performance. The main technologies used here are double and multi-effect absorption technologies.

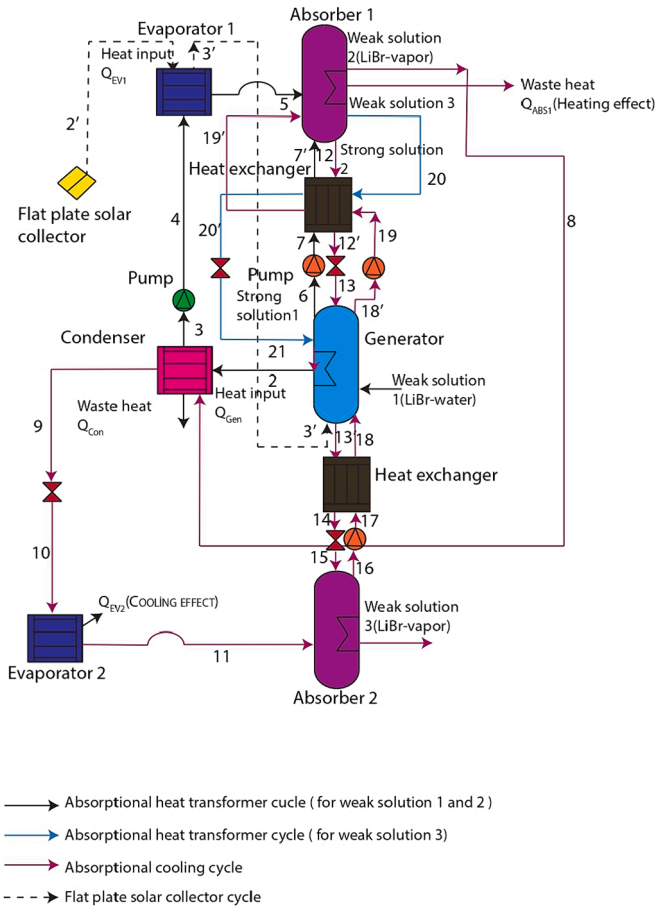

Fig. 1. Schematic description of the proposed system.

Considering the latest developments in this current research, it is clearly seen that there is a significant gap in the production of high-capacity cooling loads with simpler system design, lower cost and environmental impacts, and high cooling performance with the integration of low temperature waste heat. The current study focused on this key gap as described in the existing literature by utilizing single-stage absorption technology. In this context, a novel system, which included incorporating flat plate solar collector (FPSC), LiBr absorptional heat transformer (AHT), and absorptional cooling cycle (ACC) systems, was proposed. In this novel system, through the integration of FPSC, the AHT system was operated with lower-grade waste heat sources (70 °C-90 °C). The water at the high temperature (120 °C-150 °C) LiBr-water solution from the AHT system absorber was integrated into the cooling system by sending it directly to the condenser and reducing it to the evaporator pressure of the ACC system to produce 4000 kW of cooling duty. In this way, the use of a generator for the cooling system was avoided. Thus, the additional cost of the boiler and additional heat source for this operation were saved. On the other hand, after the completion of the cooling cycle, the solution in the generator was sent back to the AHT system absorber, enabling the completion of the AHT cycle and obtaining 4000 kW of heating duty. The technical and economic information associated with the proposed system was evaluated against that of other cooling plants of comparable scale. This novel system was modeled with Engineering Equation Solver (EES) and Transient System Simulation Software (TRNSYS), with an illustrative case centered on Izmir, Turkey. The extended exergy and sustainability analyses, along with the environmental impact assessment, were performed. For extended exergy analysis results demonstration, the novel extended exergy flow diagram was proposed to realize the effect of extended exergy components on the entire proposed system in terms of life cycle assessments. The novel

diagram included extended exergy content components, energy carriers of the proposed system, and exergy product rate streams. The primary novelties of this study are to (i) utilize the single-stage absorption technology for high-capacity cooling load production in an economical and sustainable way via enhancing COP value, (ii) eliminate the requirement of the high-grade waste heat source, (iii) utilize generator and complicated high-cost system designs for achieving high-capacity cooling loads with an absorption cooling system, (iv) meet high-capacity heating and cooling loads in an economical way, and (v) propose a novel extended exergy flow diagram for better visualization of the proposed system with extended exergy streams in terms of life cycle assessments.

2. System description and modelling

2.1. System description

The novel system developed around the concept of the FPSC, AHT, and ACC systems for the provision of high-capacity cooling and heating duties is demonstrated in Fig. 1. In this configuration, for AHT and ACC systems, the $LiBr-H_2O$ was used. 4 MW of cooling and heating duty production with this novel system was targeted. To operate this system, it was sufficient to meet the heat requirements in the generator (Gen) and AHT system evaporator (EV1) through the integration of the FPSC. Because the temperature of the FPSC could reach ($70^{\circ}C-90^{\circ}C$), it had been possible to achieve high-capacity heating and cooling loads with a low-grade waste heat source via this system. Also, with this approach, the AHT system cost was reduced. To decrease the ACC system cost, the AHT and ACC systems were integrated by utilizing the high-temperature $LiBr-H_2O$ solution from the AHT system absorber (ABS1) before the completion of the cycle. This high-temperature $LiBr-H_2O$ solution was sent directly to the condenser, and the condensed water was integrated into the ACC system evaporator. The heating duty was produced by sending the solution in the generator back to the AHT system absorber and completing the AHT cycle after the completion of the cooling cycle. In this way, the utilization of the generator in the ACC system was prevented while additional costs and heat source requirements were saved. Also, the COP value of the ACC system became higher than 1 due to the prevention of the generator in the ACC system. Gen and EV1 temperatures were chosen $80^{\circ}C$ due to the FPSC integration. ABS1, condenser (Con), ACC system evaporator (EV2), and absorber (ABS2) temperatures were determined as, $140^{\circ}C, 40^{\circ}C, 10^{\circ}C, and 25^{\circ}C$, respectively, for the aim of providing more than 40 %-50 % of the COP value for an absorptional cooling system based on the classic PV system by performing.

a parametric study. In this way, a competitive solar-powered cooling-heating system was constituted. In current cooling plants with high-capacity cooling loads, cooling duty was produced with relatively high initial investment and annual costs. Hence, it is targeted to produce high-capacity cooling and heating loads more economically and environmentally by combining ACC, FPSC, and AHT systems, which sets it apart from conventional cooling plants.

2.2. Process description

In the Gen, most of the water in the weak LiBr-water solution is boiled and sent to the Con with stream 2 to enrich the solution. The water exiting the condenser as the saturated liquid with stream 3 is sent to EV1 with stream 4 and exits from there in the saturated vapor phase. Vapor is sent to ABS1 via EV1 with stream 5. The solution, which becomes rich in absorbent in the Gen, is conveyed to the ABS1 by passing through the solution pump and heat exchanger. As a result of the mixing of the vapor and the rich solution in ABS1, a high-temperature, weak LiBr-water solution is obtained. Most of the vapor in the high-temperature solution is sent to the Con with stream 8, making the solution in ABS1 richer. The pressure of the water exiting the Con in the saturated liquid phase is reduced to the pressure of EV2 with the expansion valve at streams 9 and 10. The saturated vapor coming out of EV2 is transmitted to ABS2 with stream 11. The solution enriched in ABS1 is sent to ABS2 with streams of 12 through 15. Mixing of vapor and rich solution in ABS2, weak LiBr-water solution is obtained. By transmitting this solution to Gen with streams 16–18, ACC is completed, and thus a cooling load of 4000 kW is obtained. To obtain a heat load of 4000 kW, the AHT cycle must be completed. The weak solution transmitted to Gen with streams of 19 and 20 is sent to ABS1 by passing through the solution pump and heat exchanger. By transmitting the solution in ABS1 to Gen again with stream of 21, the AHT cycle is completed, and a heating load of 4000 kW is obtained.

Table 1
Specification of design parameter and assumptions for the proposed system.

Design parameters		Assumptions made	
AHT system	ACC system	AHT system	ACC system
Generator temperature:80 °C	Evaporator temperature: 1 0 °C	Water leaves the condenser in the saturated liquid phase.	Water leaves the condenser in the saturated liquid phase.
Condenser temperature: 4 0 °C	Absorber temperature: 25 °C	Water leaves the evaporator in the saturated vapor phase.	Water leaves the evaporator in the saturated vapor phase.
Evaporator temperature:80 °C	Solution heat exchanger temperature: 55 °C	LiBr-water solution separates the absorber at the absorber pressure and temperature.	LiBr-water solution separates the absorber at the absorber pressure and temperature.
Absorber temperature: 140 °C	Refrigerant-absorbent mixture: LiBr-water solution	LiBr-water solution separates the generator at the absorber pressure and temperature.	
Solution heat Exchanger temperature: 135 °C		Water separates the generator at the generator temperature.	
Refrigerant-absorbent mixture: LiBr-water solution		The variations of kinetic and potential energy are neglected. System operates steadily. The component's thermal dissipation into the surroundings is disregarded. Voltage variations are disregarded across all components, except for the pumps and valves.	

2.3. Flowsheet simulation

The proposed novel system was simulated using the EES, with unique assumptions and design parameters detailed in Table 1. Based on this thermodynamic model, the flowsheet simulation results are shown in Table 2.

Table 2
Flowsheet simulation results.

Stream	$P[kPa]$	T [°C]	$\dot{m}[kg/s]$	$h[kJ/kg]$	$s\left[\frac{kJ}{kgK}\right]$	$X[\%]$
0	3.17	25	0.89	104.8	0.37	
1	3.17	90	0.89	2669	8.93	
2	7.38	80	0.89	2649	8.48	
3	7.38	40	0.89	167.5	0.57	
4	47.37	80	0.89	334.9	1.08	
5	47.37	80	0.89	2643	7.61	
6	47.37	140	16.22	319.3	0.73	63.49
7	39.34	135	16.22	310.1	0.70	63.49
8	7.38	140	1.70	387.4	0.31	80.25
9	7.38	40	1.70	167.5	0.57	
10	1.23	10	1.70	167.5	8.90	
11	1.23	10	1.70	2519	8.90	
12	7.38	140	17.11	387.4	0.31	80.25
13	180.5	180.50	17.11	387.4	0.95	60.19
14	55	55	17.11	237.9	−1.91	80.25
15	110.8	110.8	17.11	237.9	0.73	50.68
16	1.23	25	18.81	45.46	0.21	46.10
17	6.07	55	18.81	113.9	0.43	46.10
18	19	80	18.81	171.3	0.60	46.10
19	137	135	18.81	299.3	0.94	46.10
20	159.3	140	18.81	311.1	0.97	46.10
21	19	80	18.81	171.3	0.60	46.10

Table 3
Comparison results of the proposed system modelling for absorptional heat transformer cycle.

Results of the experimental study		Results of the proposed system		Comparison	
COP for cooling	COP for heating	COP for cooling	COP for heating	Deviation for COP based on the cooling (%)	Deviation for COP based on the heating (%)
0.335	0.45	0.33	0.44	1.515	2.273

3. Analyses

3.1. Validation of the proposed system model

The proposed system consists mainly of an absorptional heat transformer and absorptional cooling cycles. Hence, to validate the proposed system modeling, firstly the previously published experimental studies based on these cycles from the literature were chosen [36,37], and then these results were compared to the proposed system modeling results in terms of COP for cooling and heating applications. In this comparison, the design parameters for these cycles were the same as in the chosen experimental studies. In Table 3, the comparison results are presented with the deviation percentages. The results from this table clearly show that the findings obtained from the proposed system model are quite close to the experimental results.

3.2. Energy analysis

The energy analysis of this novel system was conducted using mass and energy balance equations, as outlined in Table 4, with assumptions and design parameters specified in Table 1. In the FPSC, tilt and azimuth angles were taken as the optimum tilt and azimuth angles for the city of Izmir, Turkey, via the utilization of the TRNSYS presented by [38]. The integration of other system equipment into TRNSYS was performed by externally calling the EES model.

3.3. Exergy analyses

Exergy analysis was carried out on this system to assess the energy quality in accordance with the principles of the second law of thermodynamics. With this analysis, potential improvements comments based on the equipment can be easily developed. Hence, in the current study, conventional and cumulative exergy analyses were applied to the novel system. In these analyses, the exergy values, both physical and chemical in nature, were calculated using equations (1–3) provided in the formulae section (Tiktas et al. [39]).

Table 4
Mass and energy balance equations.

Equipment	Mass Balance Equation	Energy Balance Equation
Generator	$\dot{m}_{18} = \dot{m}_{13} + \dot{m}_{21}\dot{m}_{18}X_{18} = \dot{m}_{13}X_{13} + \dot{m}_{21}X_{21}$	$\dot{Q}_{gen} = \dot{m}_{18}h_{18} - \left[\dot{m}_{21}h_{21} + \dot{m}_{13}h_{13}\right]$
Condenser	$\dot{m}_2 = \dot{m}_3$	$\dot{Q}_{con} = \dot{m}_2(h_2 - h_3)$
Pump 1	$\dot{m}_3 = \dot{m}_4$	$\dot{m}_3h_3 + \dot{W}_{p1} = \dot{m}_4h_4$
Pump 2	$\dot{m}_6 = \dot{m}_7$	$\dot{m}_6h_6 + \dot{W}_{p2} = \dot{m}_7h_7$
Pump 3	$\dot{m}_{18} = \dot{m}_{19}$	$\dot{m}_{18}h_{18} + \dot{W}_{p3} = \dot{m}_{19}h_{19}$
Pump 4	$\dot{m}_{16} = \dot{m}_{17}$	$\dot{m}_{16}h_{16} + \dot{W}_{p4} = \dot{m}_{17}h_{17}$
Evaporator 1	$\dot{m}_4 = \dot{m}_5$	$\dot{Q}_{EV1} = \dot{m}_4(h_5 - h_4)$
Evaporator 2	$\dot{m}_{10} = \dot{m}_{11}$	$\dot{Q}_{EV2} = \dot{m}_{10}(h_{11} - h_{10})$
Absorber 1	$\dot{m}_{19'} = \dot{m}_{20} + \dot{m}_{12}\dot{m}_{19}X_{19'} = \dot{m}_{20}X_{20} + \dot{m}_{12}X_{12}$	$\dot{Q}_{AB1} = \left[\dot{m}_{20}h_{20} + \dot{m}_{12}h_{12}\right] - \dot{m}_{19'}h_{19'}$
Absorber 2	$\dot{m}_{11} + \dot{m}_{15} = \dot{m}_{16}\dot{m}_{15}X_{15} = \dot{m}_{16}X_{16}$	$\dot{Q}_{AB2} = \dot{m}_{16}h_{16} - \left[\dot{m}_{11}h_{11} + \dot{m}_{15}h_{15}\right]$
Solution heat exchanger	$\dot{m}_{12} = \dot{m}_{12'}\dot{m}_{20} = \dot{m}_{20'}\dot{m}_7 = \dot{m}_{7'}\dot{m}_{12}X_{12} = \dot{m}_{12'}X_{12'}\dot{m}_{20}X_{20} = \dot{m}_{20'}X_{20'}\dot{m}_7X_7 = \dot{m}_7X_7$	$\dot{m}_{20}h_{20} + \dot{m}_7h_7 + \dot{m}_{12}h_{12'} = \dot{m}_{20'}h_{20'} + \dot{m}_7h_7 + \dot{m}_{12}h_{12}$
Expansion valve 1	$\dot{m}_{20'} = \dot{m}_{21}$	$h_{20'} = h_{21}$
Expansion valve 2	$\dot{m}_{12'} = \dot{m}_{13}$	$h_{12'} = h_{13}$
Expansion valve 3	$\dot{m}_9 = \dot{m}_{10}$	$h_9 = h_{10}$
Expansion valve 4	$\dot{m}_{14} = \dot{m}_{15}$	$h_{14} = h_{15}$
Flat plate solar collector	$\dot{m}_1 = \dot{m}_{2'}$	$\dot{Q}_y = \dot{m}_{2'}c_p(T_{2'} - T_1)$

where $\dot{m}[kg/s], X(\%), T[^\circ C], h[kJ/kg], \dot{W}_p[kW], \dot{W}_t[kW], c_p, \dot{Q}[kW]$, and f are mass flow rate, LiBr concentration in solution, temperature, specific enthalpy for streams, pump and turbine power, specific heat of working fluid, heat transfer rate and circulation rate, respectively.

3.3.1. Traditional exergy analysis

This analysis was conducted using the exergy balance equations outlined in Table 5, enabling the determination of exergy destruction rates and exergy efficiency for each component as well as the overall system.

3.3.1.1. Extended exergy analysis. Through an extended exergy analysis, life cycle evaluations of the innovative system were carried out, considering factors such as labor, capital, and environmental considerations, using the cumulative exergy consumption approach. The extended exergy components were computed with Eqs. (4–8) given in Ref. [40]. To calculate these components, the cumulative exergy and environmental analyses were implemented with the utilization of the relevant data presented in Table 6.

3.4. Cumulative exergy consumption analysis

The cumulative exergy consumption analysis was implemented in this novel system by following the 'input–output method'. To perform this, first, energy carriers were defined for the novel system as main products, by-products, and external supplies. The definitions are shown in Table 7. Then, the mathematical model was formed based on this

Table 5
Exergy balance equations.

Equipment	Exergy Balance Equation
Generator	$\dot{E}x_{d,gen} = \dot{Q}_{gen}\left(1-\frac{T_0}{T_{gen}}\right) + \left[\dot{m}_{18}\dot{E}x_{18} - \dot{m}_{21}\dot{E}x_{21} - \dot{m}_{13}\dot{E}x_{13}\right]$
Condenser	$\dot{E}x_{d,con} = -\dot{Q}_{con}\left(1-\frac{T_0}{T_{con}}\right) + \left[\dot{m}_{2}\dot{E}x_{2} - \dot{m}_{3}\dot{E}x_{3}\right]$
Pump 1	$\dot{E}x_{d,P1} = \dot{W}_{p1} + \left[\dot{m}_{3}\dot{E}x_{3} - \dot{m}_{4}\dot{E}x_{4}\right]$
Pump 2	$\dot{E}x_{d,P2} = \dot{W}_{p2} + \left[\dot{m}_{6}\dot{E}x_{6} - \dot{m}_{7}\dot{E}x_{7}\right]$
Pump 3	$\dot{E}x_{d,P3} = \dot{W}_{p3} + \left[\dot{m}_{18}\dot{E}x_{18} - \dot{m}_{19}\dot{E}x_{19}\right]$
Pump 4	$\dot{E}x_{d,P4} = \dot{W}_{p4} + \left[\dot{m}_{16}\dot{E}x_{16} - \dot{m}_{17}\dot{E}x_{17}\right]$
Evaporator 1	$\dot{E}x_{d,EV,1} = \dot{Q}_{EV,1}\left(1-\frac{T_0}{T_{EV,1}}\right) + \left[\dot{m}_{4}\dot{E}x_{4} - \dot{m}_{5}\dot{E}x_{5}\right]$
Evaporator 2	$\dot{E}x_{d,EV,2} = \dot{Q}_{EV,2}\left(1-\frac{T_0}{T_{EV,2}}\right) + \left[\dot{m}_{4}\dot{E}x_{10} - \dot{m}_{5}\dot{E}x_{11}\right]$
Absorber 1	$\dot{E}x_{d,AB1} = -\dot{Q}_{AB1}\left(1-\frac{T_0}{T_{AB1}}\right) + \left[\dot{m}_{20}\dot{E}x_{20} + \dot{m}_{12}\dot{E}x_{12} - \dot{m}_{19'}\dot{E}x_{19'}\right]$
Absorber 2	$\dot{E}x_{d,AB2} = \dot{Q}_{AB2}\left(1-\frac{T_0}{T_{AB2}}\right) + \left[\dot{m}_{16}\dot{E}x_{16} - \dot{m}_{11}\dot{E}x_{11} - \dot{m}_{15}\dot{E}x_{15}\right]$
Solution heat exchanger	$\dot{E}x_{d,SHX} = \left(\dot{m}_{20}\dot{E}x_{20} + \dot{m}_{7}\dot{E}x_{7} - \dot{m}_{12}\dot{E}x_{12}\right)$
Expansion valve 1	$\dot{E}x_{d,V1} = \left(\dot{m}_{20'}\dot{E}x_{20'} - \dot{m}_{21}\dot{E}x_{21}\right)$
Expansion valve 2	$\dot{E}x_{d,V2} = \left(\dot{m}_{12'}\dot{E}x_{12'} - \dot{m}_{13}\dot{E}x_{13}\right)$
Expansion valve 3	$\dot{E}x_{d,V3} = \left(\dot{m}_{9}\dot{E}x_{9} - \dot{m}_{10}\dot{E}x_{10}\right)$
Expansion valve 4	$\dot{E}x_{d,V4} = \left(\dot{m}_{14}\dot{E}x_{14} - \dot{m}_{15}\dot{E}x_{15}\right)$
Flat plate solar collector	$\dot{E}x_{d,FSC} = A_k I\left(1+\frac{1}{3}\left(\frac{T_0}{T_{solar}}\right)^4 - \frac{4}{3}\frac{T_0}{T_{solar}}\right) - \left[\dot{m}_{2'}c_p(T_{2'}-T_1) - T_0 ln\left(\frac{T_{2'}}{T_1}\right)\right]$

where $T_0[K]$, $T_{solar}[K]$, $A_k\,[m^2]$, $I[kW/m^2]$, $\dot{E}x[kW]$, and $\dot{E}x_d[kW]$ are dead-state and solar temperatures, cross-sectional area of solar collector, solar radiation density coming to the collector surface, exergy rate of streams and exergy destruction rates for equipment, respectively.

Table 6
Data used for the extended exergy analysis.

N_h	84.98 Mperson
N_w	345.45 Mworker
N_{wh}	75,999 Mworkhour
Ex_{surv}	10.50 MJ/(day.person)
f	14.91

Table 7
Definition of energy carriers corresponding to the proposed system for cumulative exergy consumption analysis.

Energy carriers					
No	Main products	No	By products	No	External supplies
1	Cooling duty [MJ]	1	Generator waste heat [MJ]	1	Weak LiBr-water solution 1 stream [kg]
2	Weak LiBr-water solution 2 stream [kg]	2	Condenser waste heat[kJ]	2	Raw water stream entering the solar collector [kg]
3	Heating duty [kg]	3	Absorber 2 waste heat [MJ]		
4	Weak LiBr-water solution 3 stream [kg]				

method, and the balance equation of Eq. (9) was written in matrix form depending on the average weighted indices. In this mathematical model, the auxiliary equation of Eq. (10) was utilized due to the not lack of by-products and external supplies to the main production. The resulting vector of the cumulative exergy consumption for main products was established by solving Eqs. (9–10) presented by [41].

3.5. Environmental impact assessment

To establish the total greenhouse gas emission amount corresponding to the novel system, the environmental analysis was implemented. The direct and indirect emissions were calculated using Eqs. (11–16) provided by [42].

3.6. TRNSYS modelling of the proposed system for annual simulation

With energy and exergy analyses, the proposed system was evaluated instantly; however, this assessment did not provide a comprehensive understanding of the system's actual performance. As a result, a TRNSYS model was developed, with an illustrative example centered on the city of Izmir, to conduct annual performance simulations of the novel system. In this modeling, the FPSC component was taken directly from the TRNSYS; however, other components were integrated into the TRNSYS by calling EES.

3.7. Economic evaluation and comparison with previous similar scaled systems

An economic assessment of the proposed novel system was performed to present the effective utilization potential of the system compared to other similar-scaled systems. In this evaluation, investment cost, annual operation cost, payback period, internal rate of return, net present value, and levelized cost of cooling duty were considered. Based on the outcomes of the economic evaluation and comparative analysis, the innovative system appears to be a compelling choice, offering a robust alternative for meeting high-capacity cooling and heating requirements when compared to other systems.

3.8. Sustainability analysis

In the sustainability analysis, metrics, such as the social-ecological factor, ecological impact, and exergetic sustainability index, were calculated for the proposed innovative system. In this analysis, Eqs. (17–19) provided by [43] were used.

4. Results and discussion

4.1. Energy analysis results

In Table 8, the energy analysis findings of the proposed novel system are summarized. It is clearly shown that the heat effect coefficient of AHT and the COP value for the cooling system are 0.46 and 3.10, respectively. The COP value of 3.10 proved to reach the aim of upgrading of the COP value with lower-grade waste heat sources, which is higher than the one mentioned in the introduction section. The obtained result originated from the elimination of Gen in the ACC system by integrating the high-temperature LiBr-water solution from ABS1 into the cooling system. According to the results from this table, 19,233 m^2 of FPSC field area are required to operate the proposed system.

4.2. Exergy analysis results

In this paper, in the context of exergy, conventional, cumulative, and extended exergy analyses were performed. To implement these analyses, fuel and product exergy definitions were made. The heating and cooling duties were defined as product exergy due to being main products of the proposed system. However, pumping work was established as fuel exergy (or exergetic fuel) due to the need for this externally to operate the proposed system.

Table 8
Energy analysis results of the proposed system.

Absorptional heat transformer cycle		Absorptional cooling cycle		Flat plate solar collector system	
Circulation ratio,f	18.27	Heat transfer rate in evaporator,$\dot{Q}_{EV2}[kW]$	4000	Required heat transfer rate in collector,$\dot{Q}_y[kW]$	8678
Heat effect coefficient, $ITK[s/kJ]$	0.46	Coefficient of performance,COP	3.103	Required collector field area,$A[m^2]$	19,233
Heat transfer rate in evaporator, $\dot{Q}_{EV1}[kW]$	2050				
Required pump powers, $\dot{W}_{P,AHT}[kW]$	2704.40				
Heat transfer rate in condenser,$\dot{Q}_{con}[kW]$			2204		
Heat transfer rate in generator,$\dot{Q}_{Gen}[kW]$			6628		

Table 9
Conventional exergy analysis results of the proposed system.

Component	Product exergy rate,$\dot{E}x_P[kW]$	Fuel exergy rate,$\dot{E}x_F[kW]$	Exergy destruction rate,$\dot{E}x_D[kW]$	Exergetic efficiency,η_{ex}
Generator	994.20	1127	132.40	0.88
Condenser	110.40	140.80	30.43	0.78
Pump 1	36.43	148.70	133.10	0.11
Pump 2	36.43	148.70	133.10	0.11
Pump 3	488.60	2407.6	1919	0.20
Pump 4	58.68	1287	1228	0.05
Evaporator 1	320.10	348.40	28.30	0.92
Evaporator 2	141.30	4000	3859	0.04
Absorber 1	1162	2175	1013	0.53
Absorber 2	187.50	1136	948.80	0.17
Solution heat exchanger	8695	9184	488.60	0.946
Expansion valve 1	8695	9241	545.80	0.941
Expansion valve 2	11,422	13,053	1631	0.88
Expansion valve 3	2.36	2.43	0.06	0.98
Expansion valve 4	8768	9840	1071	0.89
Flat plate solar collector	14.37	1295	1281	0.01
Heating subsystem				0.82
Cooling subsystem				0.76
Solar collector subsystem				0.011
Overall system				0.74

4.2.1. Traditional exergy analysis results

In Table 9 and Fig. 2, the conventional exergy analysis conclusions corresponding to the proposed system are presented. It was clearly stated in Table 6 that for this system, the entire exergy destruction rate was 14442.59 kW. EV2, P3, and V2 were the highest contributors to the overall system exergy destruction rate, with 26.72 %, 13.29 %, and 11.29 %, respectively. However, the lowest contributors were Con, EV1, and V3, with rates of 0.21 %, 0.20 %, and 0.0004 %, respectively. This situation originated from the existence of effective thermal reactions in these components.

The exergy flow and loss diagram (also called the Grassmann diagram) based on the traditional exergy analysis results is demonstrated in Fig. 3, where exergy destruction and fuel rates are visualized for each individual component of the proposed system by utilizing of an effective scale.

The traditional exergy analysis results clearly show that the components of EV2, P3, and V2 must be prioritized for improvement of the overall system from the thermodynamic point of view. In these components, the exergy fuel rate is quite higher compared to the exergy product rate. Because the primary fuel rates related to thermal and chemical reactions existed in these components. This situation occurred in EV2 due to the increasing heat transfer rate based on the higher cooling load production requirement. The main reason for this occurrence in P3 is the enhancing enthalpy difference in P3 related to the LiBr concentration with the exchanging process of solution. However, in V2, the exergy destruction rate is higher due to the enhanced entropy change based on the requirement of keeping the enthalpy the same throughout the process with the decreasing temperature related to the exchanging process. Considering all these situations, it is clear that the exergy fuel rate must be reduced in this component for approximately the same exergy product rate in order to improve the entire system. In order for this to be achieved, the reasons just mentioned must be alleviated. To reduce the effect of the situation in EV2, a parametric study concluded

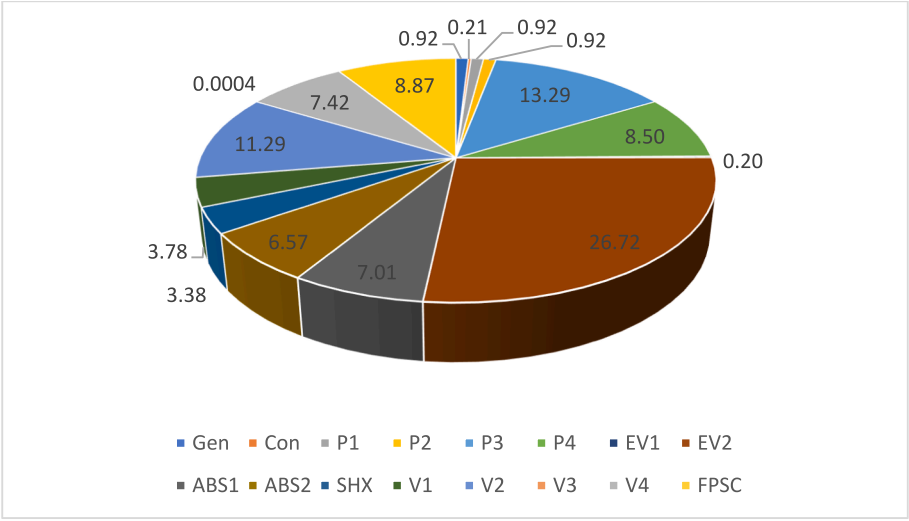

Fig. 2. Exergy destruction rate distribution of the overall system for each component in terms of percentile.

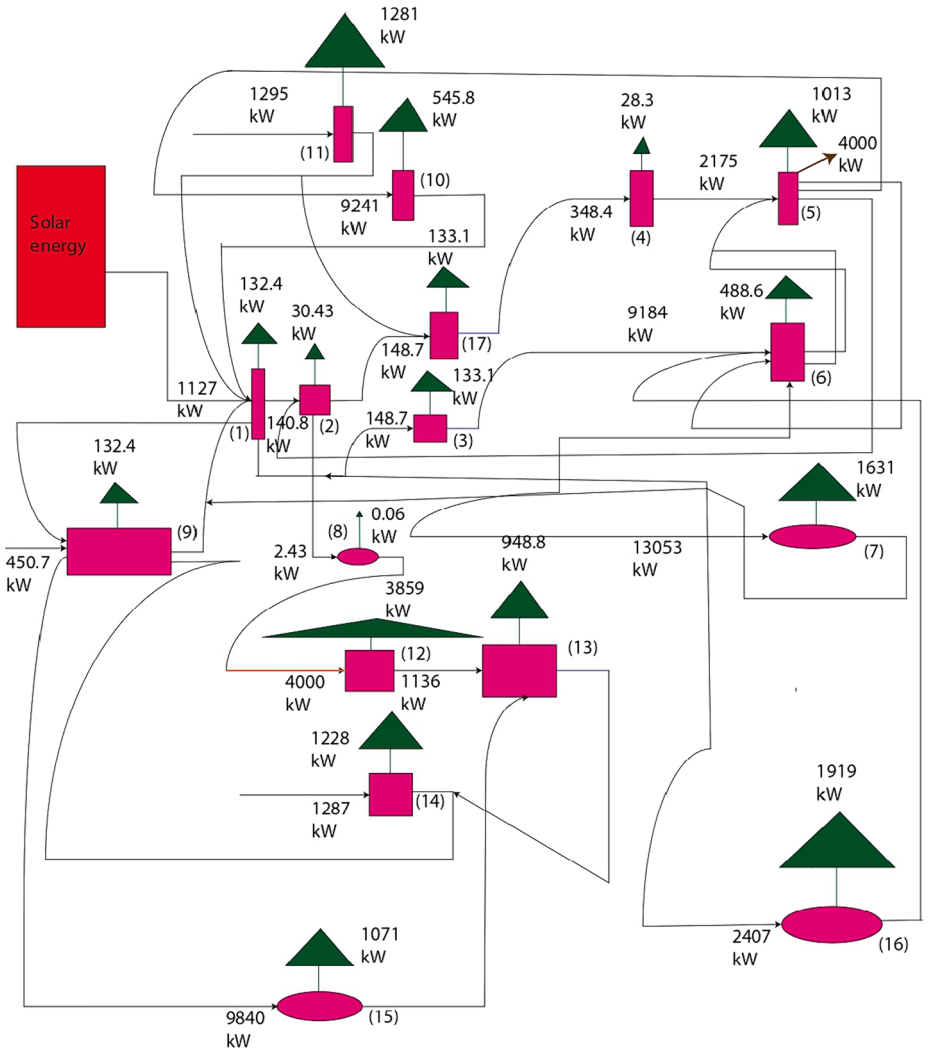

Fig. 3. Exergy flow and loss (Grassmann) diagram of the proposed system based on the conventional exergy analysis results.

that the temperature of this component should be reduced. This change results in the reduced pumping work in the ACC system, increased heat transfer rates in Gen and EV1, and a decrease in the exergy product rate due to the decrease in the temperature of EV2. The main effect causing this change is the decrease in the mass flow rate of the working fluid entering from ABS2 to EV1. On the other hand, it is recommended to increase the ABS2 temperature for P3 and V2, where the process of replacing solutions of different concentrations with each other occurs intensively. This change results in the reduced pumping work in the ACC system and increased heat transfer rates and exergy fuel rates in Gen and EV1. This change will be possible by decreasing the mass flow rate of the working fluid, leaving ABS2 and entering EV1. In summary, in this study, it is recommended to reduce the EV2 temperature and increase the ABS2 temperature through parametric optimization to improve the entire system. It has been clearly seen that if this optimization is made, the proposed system can achieve the desired cooling and heating load with lower pumping work.

Table 10
Extended exergy analysis results of the proposed system.

ee_L	63.89 MJ/workhour
E_L	4.86 GJ
ee_c	38.85 MJ/€
E_C	13.88 GJ
E_E	8.538x 10^{-3} GJ
$E^{cum,ex}{}_{cool}$	2724280.74 GJ
$E^{cum,ex}{}_{heat}$	1497801.60 GJ
$E_{cum,T}$	4222082.34 GJ
EE	4222101.09 GJ
EXP	1,842,120 GJ
EED	2379981.09 GJ
Φ_{EE}	0.44

4.2.1.1. Extended exergy analysis results. In Table 10, the extended exergy analysis findings for the proposed system are presented. From the results of the table, the total extended exergy content is 4222101.09 GJ,

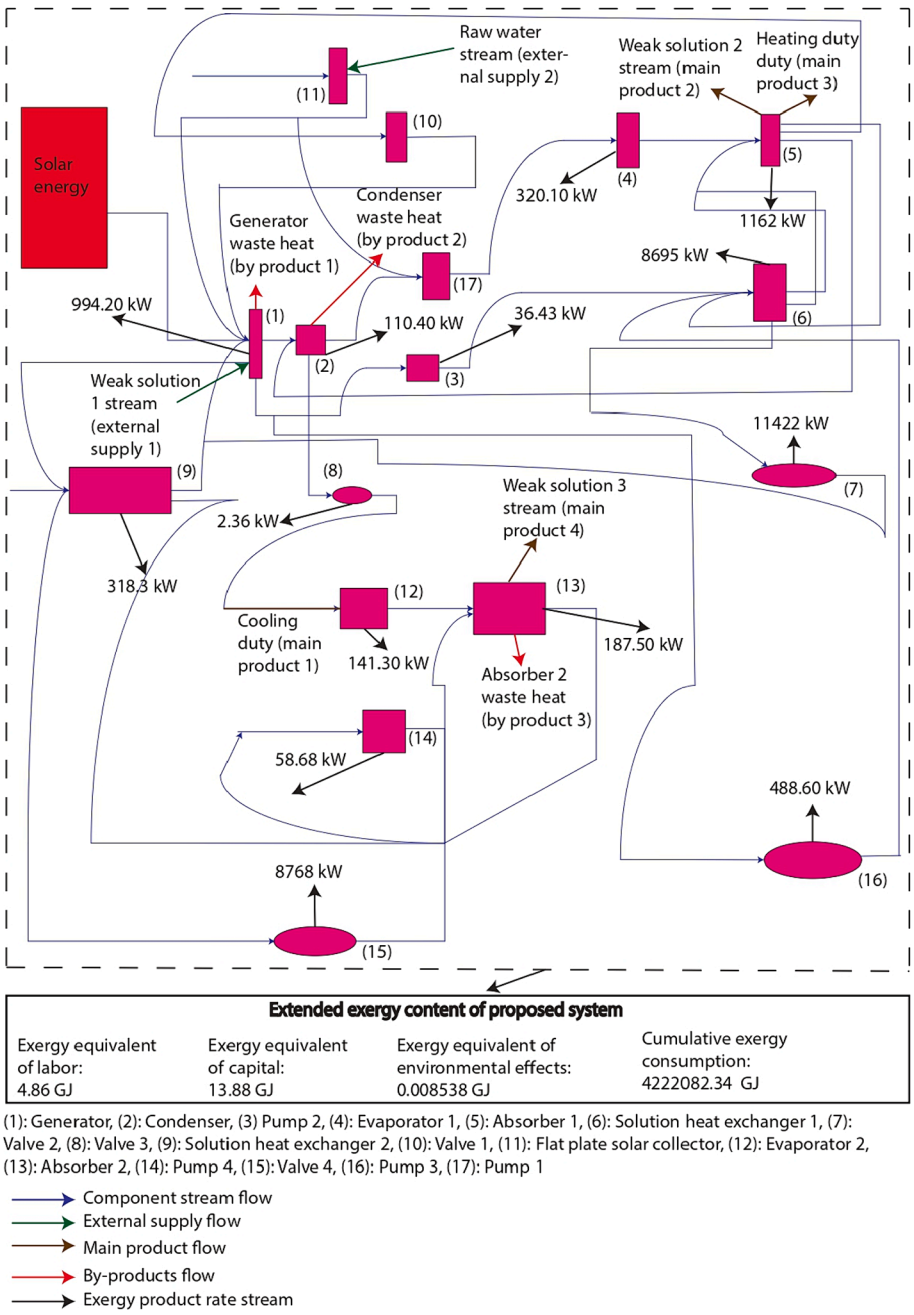

Fig. 4. Novel extended exergy flow diagram for the proposed system based on the extended exergy analysis results.

and the cumulative exergy consumption component becomes the most contributor to this compared to the capital, labor, and environmental remediation cost components. This situation shows that in this proposed system for provision of high-capacity cooling and heating loads, the highest consumption occurred in material and energy. Other consumptions associated with the cost of investment, electricity, and environmental remediation become lower due to the relatively lower electricity consumption of pumps compared to the main product generation. This result proves the approach to the aim of enhancing the economic viability of the proposed system for high-capacity cooling and heating load provision. Another important conclusion from Table 10 is the extended exergy efficiency was 43.6 % lower than conventional exergy efficiency of 74.1 %. This result originated from the utilization of exergy fuel components apart from the energy content in the extended exergy analysis considerations. In the extended exergy analysis, it is worth noting that the exergy product rate remained consistent with the conventional exergy analysis approach. But the exergy destruction rate was higher in the extended exergy analysis than the conventional one. The novel extended exergy flow diagram for the proposed system is presented in Fig. 4 where energy carriers of the proposed system are classified and demonstrated as main products, by-products, and external supplies. In addition to this, the exergy product rate of each component of the proposed system and the extended exergy content components for the entire system are visualized in Fig. 4. In this way, the proposed system was comprehensively demonstrated in terms of life cycle assessments. The general methodology of the novel extended exergy flow diagram is given in Table 11.

4.3. *Annual simulation results in TRNSYS modelling*

TRNSYS simulation results for annual heating and cooling duty generation are presented in Fig. 5. Based on the simulation results, the

Table 11
General methodology of the novel extended exergy flow diagram.

Step 1: Constitute thermodynamic model of the proposed system.

↓

Step 2: Firstly apply energy and conventional exergy analysis on the system and determine exergy product and destruction rates for each equipment.

↓

Step 3: Estimate the energy carriers and materials for system as main products, by-products and external supplies.

↓

Step 4: According to the energy carriers and materials, apply extended exergy analysis on the system.

↓

Step 5: From the extended exergy analysis results, determine the exergy equivalent of labor, capital, environmental effects and cumulative exergy consumption

↓

Step 6: Relate the exergy equivalents and energy carriers and materials.

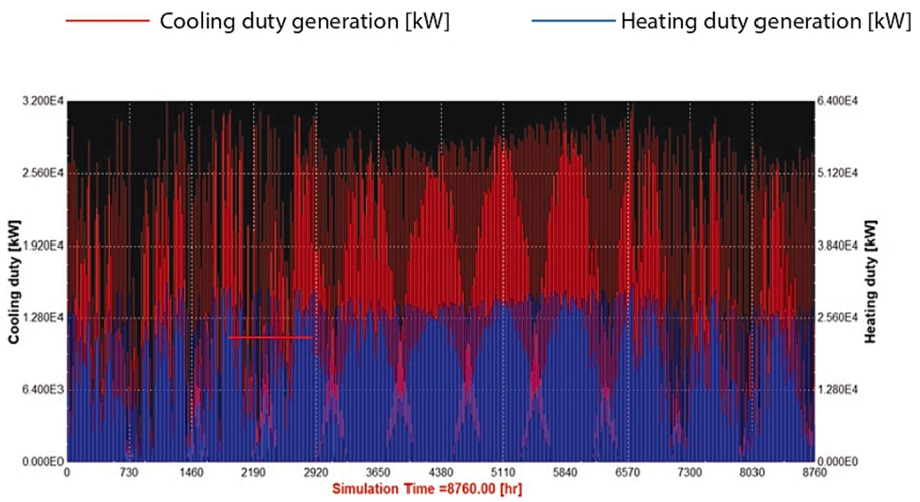

Fig. 5. Annual heating and cooling duty generation simulation corresponding to the proposed system in TRNSYS for an illustrative example of Izmir, Turkey.

entire annual cooling and heating duty generations were determined to be 52,370 MWh and 52,400 MWh, respectively. Figs. 6-11 illustrate the variation of heat effect coefficient (HEC) for the AHT system, COP for the ACC system, exergy product rate, extended exergy rate, and extended and conventional exergy efficiency for the proposed system annually. According to Figs. 6-7, the highest HEC and COP values during the year were 0.46 and 3.11, respectively. Also, in these figures, it is shown that with increasing the solar radiation density, HEC and COP values decrease monotonically. This situation can be explained by the fact that more exergetic fuel is required to achieve the same heating and cooling outputs due to the enhanced solar radiation density, pumping works, and AHT and ACC systems heat input. The increasing solar radiation density leads to the enhancing mass flow rates in the AHT and ACC system components. However, for COP, the increasing rate of pumping work becomes higher than cooling duty. Hence, the COP value dropped monotonically with increasing the solar radiation density. Similar behavior is valid for the HEC variation. In this context, the highest decreasing and increasing rates of the HEC and COP occurred in July and August, respectively. From Figs. 8-11, it is obvious that, until August, with increasing the solar radiation density and temperature of the waste heat source, the exergy product rate and extended exergy rate increase monotonically. However, after August, this behavior was reversed. Hence, the highest values for these terms were obtained in August. However, in this month, the extended exergy rate became higher than exergy product rate. This situation originated from the inclusion of the extended exergy rate for more fuel inputs, such as capital, labor, environmental, and cumulative exergy consumption, compared to the traditional exergy analysis. At the same time, the exergy product rate was taken the same as with conventional exergy analysis. Hence, the lowest extended exergy efficiency was obtained in this month. However, August became the month with the highest conventional exergy efficiency during the year.

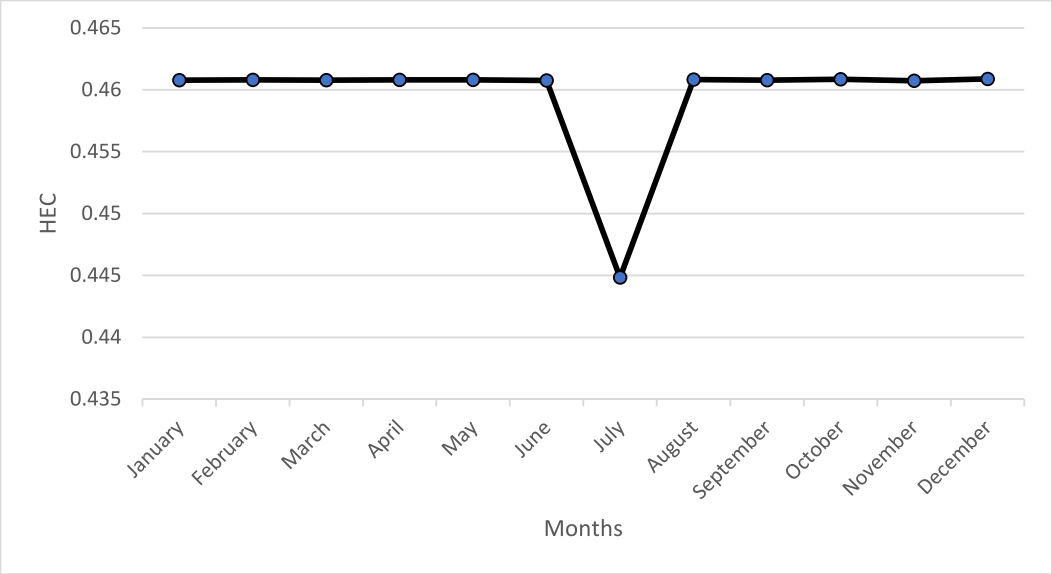

Fig. 6. Variation of HEC for the AHT system during the year.

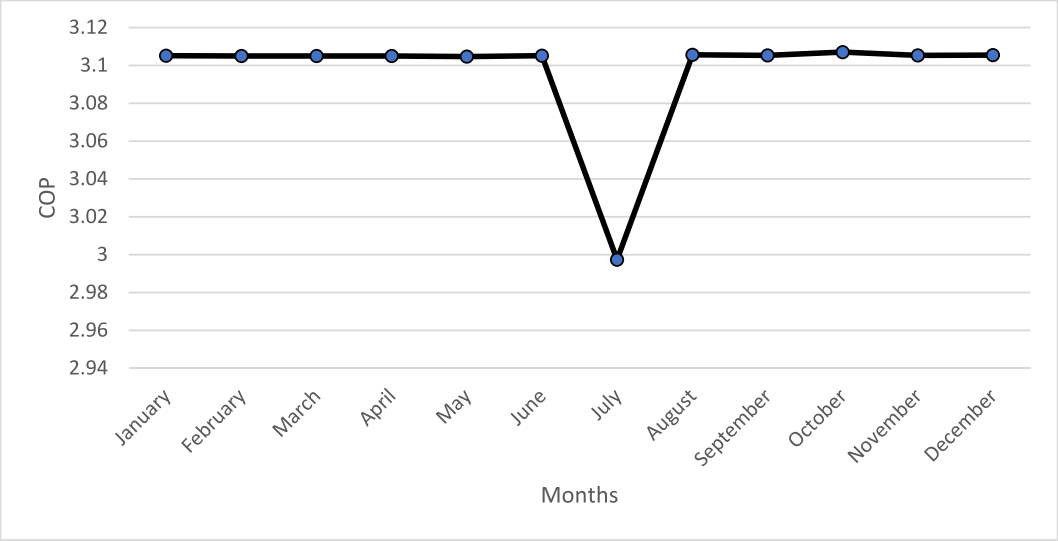

Fig. 7. Variation of COP for the ACC system during the year.

4.4. Economic evaluation results and comparison with existing medium–high scaled cooling plants

In Table 12, the economic evaluation results corresponding to the proposed system are summarized. To compare the proposed system with similar scaled cooling plants in terms of economic considerations, the reference study of Schüppler et al. [24] and the reports of the Bowling Green State University central cooling [25], Cleveland Hopkins International airport chilled water [26], and ZEOSOL integrated solar heating and cooling plants [27] were evaluated for 4000 kW of cooling duty generation. It has been determined clearly from this comparison that in the existing cooling plants for 4000 kW of cooling duty generation, the initial total investment and annual operation costs are in the range of US $6–8 million and US$5–7 million, respectively. Also, the variation in payback periods ranged from 5 to 10 years. However, the economic parameters of initial total investment, and annual operation costs, and payback period for the proposed system were US$4.56 million, US$3.12 million, and 1.75 years, respectively. The results showed that, in addition to the 4000 kW of cooling load produced in the comparison systems, a heating load of 4000 kW was produced with the proposed system at a lower cost than the existing systems. The annual energy cost gain of the proposed system was also determined to be US$3.89 million. This comparison clearly indicates that the integration of FPSC, AHT, and ACC with the proposed system has provided a stronger alternative to the existing cooling-heating cogeneration systems more economically.

4.5. Environmental impact and sustainability analysis findings

In Tables 13 and 14, the sustainability and environmental analysis findings are demonstrated, respectively. In these tables, it has been clearly shown that the levelized cooling duty generation capacity equivalent CO_2 emission is 0.201 t/MWh. Previous literature studies on medium–high-capacity cooling plants indicated that this value was in the range of 0.4 and 0.6 for 4000 kW of cooling duty generation [44,45]. This result shows that the proposed system presents a superior alternative in terms of exergo-environmental considerations when compared to existing medium–high-capacity cooling plants.

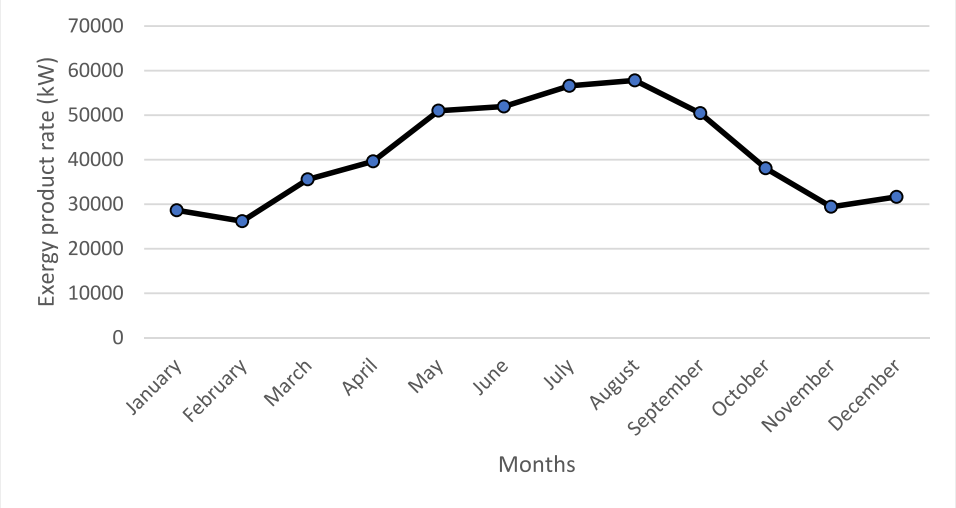

Fig. 8. Variation of exergy product rate during the year.

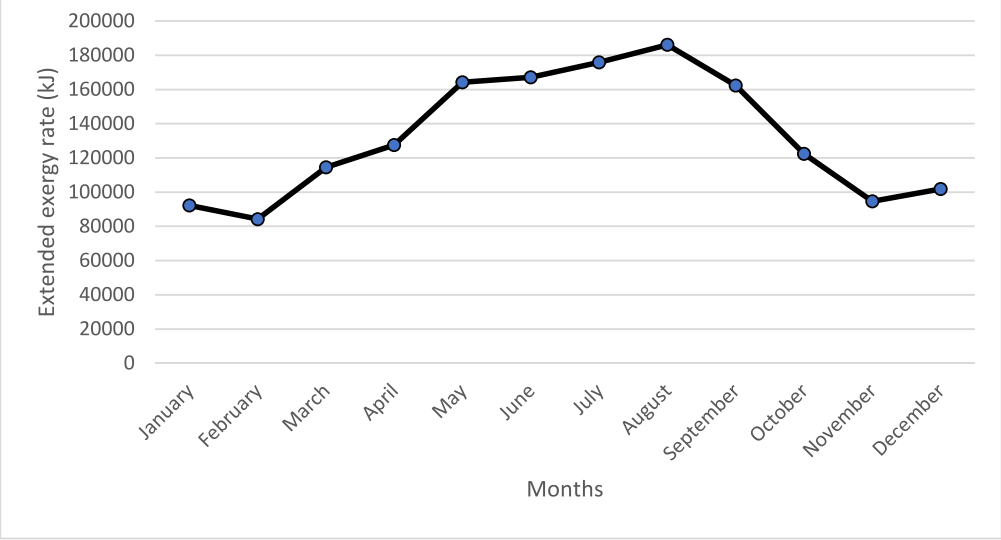

Fig. 9. Variation of extended exergy rate during the year.

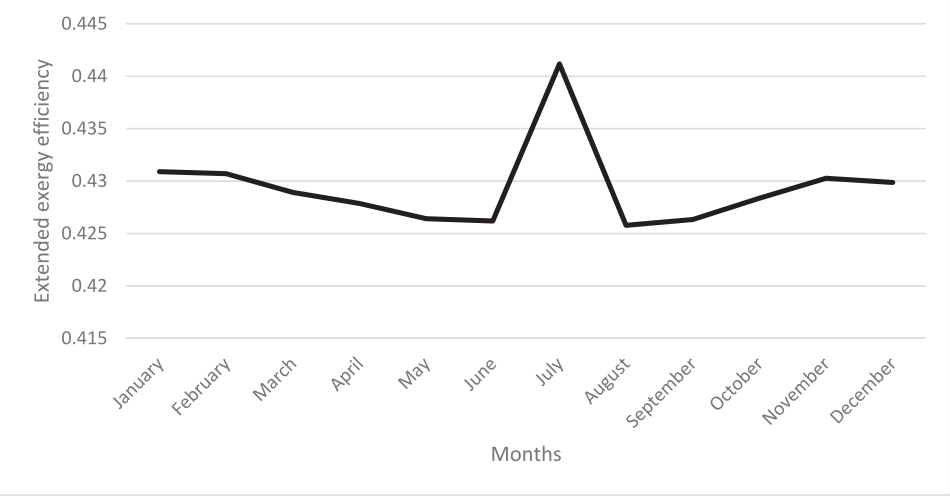

Fig. 10. Variation of extended exergy efficiency during the year.

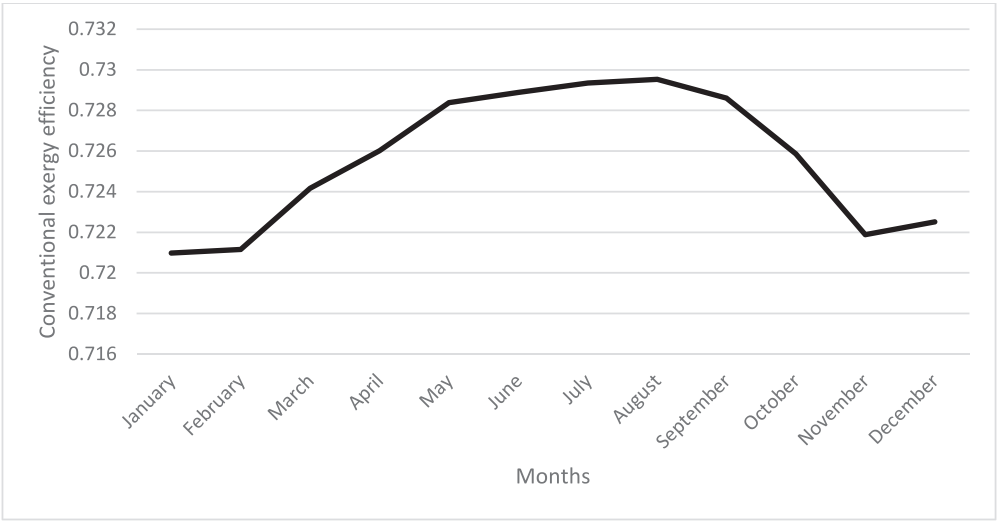

Fig. 11. Variation of conventional exergy efficiency during the year.

Table 12
Economic evaluation results of the proposed system.

Cost of absorptional heat transformer cycle	US$1.74 million
Cost of absorptional cooling cycle	US$900.42 thousand
Installed cost of flat plate solar collector	US$96/$m^2$
Total direct cost	US$4.49 million
Total indirect cost	US$673.38 thousand
Total cost	US$4.56 million
Payback period	1.748 years
Net present value	US$19.62 million
Internal rate of return	20.39 %
Levelized cost of cooling capacity	US$0.09 /kWh
Annual operation cost	US$3.12 million
Annual energy gain cost	US$3.89 million

Table 13
Environmental impact analysis results of the proposed system.

Entire CO_2 emission corresponding to the proposed system (kg)	10501.82
Levelized cooling duty generation capacity equivalent CO_2 emission (t/MWh)	0.201
Levelized heating duty generation capacity equivalent CO_2 emission (t/MWh)	0.200

5. Conclusions

In the present study, a novel heating–cooling cogeneration system was conceptualized, incorporating FPSC, AHT, and ACC systems to harness low-grade solar energy. In this study, through this novel cogeneration system design, the aim was to achieve the generation of high-capacity cooling and heating duties through absorption technology, with a focus on improved economic efficiency and higher COP values, all while bypassing the need for high-temperature waste heat sources. In this context, the proposed system has a different behavior from the existing medium–high-capacity cooling plants. In modeling the proposed system, EES and TRNSYS were used for 4000 kW of cooling and heating duty generation by exemplifying a case study centered on Izmir, Turkey. The proposed system was compared to similar-scale cooling plants around the world. The comparison results clearly show that the proposed system stands out with a lower payback period, and initial investment, and annual operation costs compared to the existing similar-scale cooling plants. Thus, the novel system constitutes a robust alternative to the existing cooling-heating cogeneration systems in terms of main output generation and economic and environmental considerations. The novel system was evaluated by performing energy, conventional, and extended exergy and sustainability analyses, along with the environmental impact assessment. The conventional exergy analysis findings were summarized with the exergy flow and loss diagram. Also, according to the extended exergy analysis findings, the novel extended exergy flow diagram was proposed and drawn for the proposed system. In this way, an effective visualization method was implemented in terms of life cycle assessments with all components of extended exergy streams. The main concluding remarks are listed as follows:

Table 14
Sustainability analysis results of the proposed system.

Component	Ecological effect factor, *EcoEF*	Environmental effect factor,*EEF*	Exergetic sustainability index,*EXSI*	Social ecological factor,*SEF*
Generator	1.13	0.13	7.51	8.48
Condenser	1.28	0.28	3.63	4.63
Pump 1	9.52	8.53	0.12	1.12
Pump 2	9.52	8.53	0.12	1.12
Pump 3	4.93	3.93	0.26	1.26
Pump 4	21.74	20.74	0.05	1.05
Evaporator 1	1.09	0.09	11.31	12.35
Evaporator 2	28.57	27.56	0.04	1.04
Absorber 1	1.87	0.87	1.15	2.15
Absorber 2	6.06	5.06	0.20	1.20
Solution heat exchanger	1.05	0.05	17.80	18.80
Expansion valve 1	1.06	0.06	15.93	16.95
Expansion valve 2	1.14	0.14	7	8
Expansion valve 3	1.02	0.00003	39.30	40.16
Expansion valve 4	1.12	0.12	8.19	9.18
Flat plate solar collector	90.91	89.93	0.01	1.01
Overall system	1.35	0.34	2.97	3.86

a) Energy analysis results have indicated that the heat effect coefficient of AHT, COP value for the cooling system, and the required FPSC field area are 0.46, 3.10, and 19,233 m^2 respectively. The COP value above one was obtained with the elimination of Gen in the ACC system via integration of the high-temperature LiBr-water solution and the ACC system.
b) Based on exergy analysis results, for the proposed system, 14442.59 kW of the entire exergy destruction rate exists. The highest contributions to the total exergy destruction rate belonged to EV2, P3, and V2 due to the effective thermal reactions in these components, with rates of 26.72 %, 13.29 %, and 11.29 %, respectively.
c) According to extended exergy analysis results, the total extended exergy content is 4222101.09 GJ for the proposed system. The cumulative exergy consumption component has become the most contributor to the total exergy content. This result has indicated that with the novel system, capital, consumption especially based on the installation and electricity, becomes lower than material and energy consumption. Thus, these results are significant evidence for enhancing the economic viability of the proposed system based on its high-capacity cooling and heating duty generation. Based on the extended exergy, the extended and conventional exergy efficiencies are 43.60 % and 74.10 %, respectively. The extended exergy efficiency decreased in comparison to the conventional efficiency, primarily because of the higher exergy fuel rate, even though the exergy product rate remained the same.
d) The annual cooling and heating duty generations are determined as 52,370 MWh and 52,400 MWh, respectively, from TRNSYS simulation results.
e) The economic comparison results for the proposed system in relation to similar-scaled cooling plants indicate that it offers a cost-effective alternative for meeting high-capacity cooling and heating demands.
f) The novel extended exergy flow diagram was proposed and drawn for the proposed system to provide a better visualization of the system in terms of life cycle assessments with all details.

$$\dot{E}^{Ph} = \dot{m}[(h_i - h_0) - T_0(s_i - s_0)] \tag{1}$$

$$\dot{E}^{Ch} = \sum z_i b_i \tag{2}$$

$$\dot{E} = \dot{E}^{Ph} + \dot{E}^{Ch} \tag{3}$$

$$EE = E_L + E_C + E_E + E_{CEXC} \tag{4}$$

$$E_L = ee_L N_{wh} \tag{5}$$

$$ee_L = \frac{365 N_h Ex_{surv} f}{N_{wh}} \tag{6}$$

$$E_C = ee_c \sum CC \tag{7}$$

$$ee_c = \frac{365 N_h Ex_{surv} f}{S} \tag{8}$$

$$A_G{}^T ex^* + A_D{}^T ex_{DD}{}^* = ex_G{}^{*T} + \left(F^T - A_F{}^T\right) ex_F{}^* \tag{9}$$

$$ex^* = ex_G{}^* \tag{10}$$

$$Em_{direct} = C(L_T(ALR)(EOL))(GWP + adp.GWP) \tag{11}$$

$$Em_{indirect} = Em_{energy} + Em_{eq.mfg} + Em_{eq.rcy} + Em_{re.mfg} \tag{12}$$

$$Em_{energy} = LT(AEC)EF \tag{13}$$

$$Em_{eq.mfg} = \sum MM(m) \tag{14}$$

$$Em_{eq.rcy} = \sum RM(mr) \tag{15}$$

$$Em_{re.mfg} = (C + (C(ALR)(LT)))RMF + C(1 - EOL)(RDF) \tag{16}$$

$$EEF_k = \frac{FExWR_k}{\eta_{ex,k}} \tag{17}$$

$$SEF_k = \frac{1}{1 - \eta_{ex,k}} \tag{18}$$

$$ExSI_k = \frac{1}{EEF_k} \tag{19}$$

Financial funding and support

This research did not receive any specific grant from funding agencies in the public, commercial, or not-for-profit sectors.

CRediT authorship contribution statement

Asli Tiktas: Writing – original draft, Methodology, Investigation, Formal analysis, Data curation, Conceptualization. **Huseyin Gunerhan:** Writing – review & editing, Supervision, Methodology, Conceptualization. **Arif Hepbasli:** Writing – review & editing, Supervision, Methodology, Conceptualization. **Emin Açıkkalp:** Writing – review & editing, Supervision, Methodology, Conceptualization.

Declaration of competing interest

The authors declare that they have no known competing financial interests or personal relationships that could have appeared to influence the work reported in this paper.

Data availability

Data will be made available on request.

Acknowledgments

The authors are very grateful to the reviewers and editor for their valuable and constructive comments, which led to increasing the quality of the paper.

References

[1] bp. bp Energy Outlook 2023, https://www.bp.com/content/dam/bp/business-sites/en/global/corporate/pdfs/energy-economics/energy-outlook/bp-energy-outlook-2023.pdf, Access date: Jan 13, 2024.
[2] International Energy Agency. World energy outlook 2012. Paris: IEA Publications; 2012.
[3] Elnagar E, Zeoli A, Rahif R, Attia S, Lemort V. A qualitative assessment of integrated active cooling systems: a review with a focus on system flexibility and climate resilience. Renew Sustain Energy Rev 2023;175:113179.
[4] Nikbakhti R, Wang X, Hussein AK, Iranmanesh A. Absorption cooling systems–review of various techniques for energy performance enhancement. Alex Eng J 2020;59(2):707–38.
[5] Abedrabboh O, Koc M, Biçer Y. Modelling and analysis of a renewable energy-driven climate-controlled sustainable greenhouse for hot and arid climates. Energ Conver Manage 2022;273:116412.
[6] Wang M, et al. Energy performance comparison between power and absorption refrigeration cycles for low grade waste heat recovery. ACS Sustain Chem Eng 2018;6(4):4614–24.
[7] Tiktas A, et al. Exergy-based techno-economic and environmental assessments of a proposed integrated solar powered electricity generation system along with novel prioritization method and performance indices. Process Saf Environ Prot 2023;178:396–413.
[8] Wang M, Deng C, Wang Y, Feng X. Exergoeconomic performance comparison, selection and integration of industrial heat pumps for low grade waste heat recovery. Energ Conver Manage 2020;207:112532.
[9] Tan Z, Feng X, Yang M, Wang Y. Energy and economic performance comparison of heat pump and power cycle in low grade waste heat recovery. Energy 2022;260:125149.
[10] Mousavi SA, Mehrpooya MA. Comprehensive exergy-based evaluation on cascade absorption-compression refrigeration system for low temperature applications-

exergy, exergoeconomic, and exergoenvironmental assessments. J Clean Prod 2020;246:119005.
[11] Alsagri AS, Alrobaian AA, Almohaimeed SA. Concentrating solar collectors in absorption and adsorption cooling cycles: an overview. Energ Conver Manage 2020;223:113420.
[12] Singh UR, Kaushik AS, Bhogilla SS. A novel renewable energy storage system based on reversible SOFC, hydrogen storage, rankine cycle and absorption refrigeration system. Sustainable Energy Technol Assess 2022;51:101978.
[13] Abed AM, et al. Techno-economic analysis of dual ejectors solar assisted combined absorption cooling cycle. Case Studies in Thermal Engineering 2022;39:102423.
[14] Chakravarty KH, et al. A review on integration of renewable energy processes in vapor absorption chiller for sustainable cooling. Sustainable Energy Technol Assess 2022;50:101822.
[15] Mungyeko B, Baby-Jean R, Mansouri R, Ilınca A. Diffusion absorption refrigeration systems: an overview of thermal mechanisms and models. Energies 2023;16(9):3610.
[16] Zhou T, et al. Energy-exergy-economic-environmental (4E) analysis and multi-objective optimization of a cascade LiBr/H2O refrigeration and organic rankine cycle integrated system for power generation. Appl Therm Eng 2023;225:120142.
[17] Xue X, et al. Performance evaluation and exergy analysis of a novel combined cooling, heating and power (CCHP) system based on liquid air energy storage. Energy 2021;222:119975.
[18] César JC, et al. A new computational tool for the development of advanced exergy analysis and LCA on single effect LiBr–H 2 O Solar absorption refrigeration system. Lubricants 2021;9(8):76.
[19] Musharavati FK, Tarıq R. Comparative exergy, multi-objective optimization, and extended environmental assessment of geothermal combined power and refrigeration systems. Process Saf Environ Prot 2021;156:438–56.
[20] Caliskan H, et al. Advanced, extended and combined extended-advanced exergy analyses of a novel geothermal powered combined cooling, heating and power (CCHP) system. Renew Energy 2023;206:125–34.
[21] Mohan G, et al. Development of natural gas fired combined cycle plant for tri-generation of power, cooling and clean water using waste heat recovery: techno-economic analysis. Energies 2014;7(10):6358–81.
[22] Kumar P, Singh O. Thermoeconomic analysis of SOFC-GT-VARS-ORC combined power and cooling system. Int J Hydrogen Energy 2019;44(50):27575–86.
[23] Wang J, et al. Thermodynamic analysis of a combined cooling, heating, and power system integrated with full-spectrum hybrid solar energy device. Energ Conver Manage 2021;228:113596.
[24] SCHÜPPLER, Simon, et al. Cooling supply costs of a university campus. Energy 2022;249:123554.
[25] BOWLING GREEN STATE UNIVERSITY - CENTREX CENTRAL CHILLER PLANT – HAWA 2016; Accessed: Oct. 12, 2023. [Online]. Available: file:///F:/Solar+ABSHeatCool%20Research%20Article/07.10.2023/BOWLING%20GREEN%20STATE%20UNIVERSITY%20-%20CENTREX%20CENTRAL%20CHILLER%20PLANT%20-%20HAWA.html.
[26] Chilled Water Plant Assessment & Criteria Design Cleveland Airport System 2016; Accessed: Oct. 12, 2023. [Online]. Available: https://www.clevelandairport.com/sites/default/files/11_20_2018_osborn_report.pdf.
[27] Integrated solar heating and cooling unit based on a novel zeolite chiller and heat pump 2020; Accessed: Oct. 12, 2023. [Online]. Available: https://cordis.europa.eu/project/id/760210.
[28] Zhang H, et al. Energy, exergy, economic and environmental analyses of a cascade absorption-compression refrigeration system using two-stage compression with complete intercooling. Appl Therm Eng 2023;225:120185.
[29] Abam FI, et al. Thermodynamic and economic analysis of a Kalina system with integrated lithium-bromide-absorption cycle for power and cooling production. Energy Rep 2020;6:1992–2005.
[30] Gado MG, et al. Hybrid sorption-vapor compression cooling systems: a comprehensive overview. Renew Sustain Energy Rev 2021;143:110912.
[31] Yazdi M, Reza M, et al. Comparison of gas turbine inlet air cooling systems for several climates in Iran using energy, exergy, economic, and environmental (4E) analyses. Energ Conver Manage 2020;216:112944.
[32] Razmi A, et al. Thermodynamic and economic investigation of a novel integration of the absorption-recompression refrigeration system with compressed air energy storage (CAES). Energ Conver Manage 2019;187:262–73.
[33] Mortadi M, El Fadar A. Performance, economic and environmental assessment of solar cooling systems under various climates. Energ Conver Manage 2022;252:114993.
[34] Kadam ST, et al. Thermo-economic and environmental assessment of hybrid vapor compression-absorption refrigeration systems for district cooling. Energy 2022;243:122991.
[35] Zun MT, et al. Towards techno-economics of green hydrogen as a primary combustion fuel for recreational vehicle vapor absorption refrigeration system. Sustainable Energy Technol Assess 2023;56:103007.
[36] Cudok F, Ciganda JC, Kononenko N, Drescher E. Experimental results of an absorption heat transformer. In: In *12th IEA Heat Pump Conference*; 2017. p. 1–12.
[37] Marc O, Lucas F, Sinama F, Monceyron E. Experimental investigation of a solar cooling absorption system operating without any backup system under tropical climate. Energ Buildings 2010;42(6):774–82.
[38] Tiktaş A, Gunerhan H, Hepbasli A. Exergy and sustainability-based optimisation of flat plate solar collectors by using a novel mathematical model. Int J Exergy 2023;42(2):192–215.
[39] Tiktas A, Gunerhan H, Hepbasli A. Single and multigeneration rankine cycles with aspects of thermodynamical modeling, energy and exergy analyses and optimization: a key review along with novel system description figures. Energy Conversion and Management: X 2022;14:100199.
[40] Sciubba E. Beyond thermoeconomics? the concept of extended exergy accounting and its application to the analysis and design of thermal systems. Exergy, an international journal 2001;1(2):68–84.
[41] Szargut J, Zięb ik A. Fundamentals of thermal engineering (in polish). PWN 2000.
[42] Hwang Y, Ferreira CI, Piao CC. Guideline for life cycle climate performance. *International Institute of Refrigeration 2015; Paris*.
[43] Balli O, Caliskan H. On-design and off-design operation performance assessmentsof an aero turboprop engine used on unmanned aerial vehicles (UAVs) in terms of aviation, thermodynamic, environmental and sustainability perspectives. Energ Conver Manage 2021;243:114403.
[44] Hashemian N, Noorpoor A. A geothermal-biomass powered multi-generation plant with freshwater and hydrogen generation options: thermo-economic-environmental appraisals and multi-criteria optimization. Renew Energy 2022;198:254–66.
[45] Shakibi H, et al. Exergoeconomic appraisement, sensitivity analysis, and multi-objective optimization of a solar-driven generation plant for yielding electricity and cooling load. Process Saf Environ Prot 2023;170:89–111.